New CTA Protocol and 2D-3D Registration Method for Liver Catheterization

Martin Groher[1], Nicolas Padoy[1], Tobias F. Jakobs[2], and Nassir Navab[1]

[1] Chair for Computer Aided Medical Procedures (CAMP), Technische Universität München, Germany
{groher, padoy, navab}@cs.tum.edu
[2] Institute for Clinical Radiology, University of Munich, Grosshadern Hospital
tobias.jakobs@med.uni-muenchen.de

Abstract. 2D-3D registration for angiographic liver interventions is an unsolved problem mainly because of two reasons. First, a suitable protocol for Computed Tomography Angiography (CTA) to contrast liver arteries is not used in clinical practice. Second, an adequate registration algorithm which addresses the difficult task of aligning deformed vessel structures has not been developed yet. We address the first issue by introducing an *angiographic* CT scanning phase and thus create a strong link between radiologists and interventionalists. The scan visualizes arteries similar to the vasculature captured with an intraoperative C-arm acquiring Digitally Subtracted Angiograms (DSAs). Furthermore, we propose a registration algorithm using the new CT phase that aligns arterial structures in two steps: a) Initialization of one corresponding feature using vessel diameter information, b) optimization on three rotational and one translational parameter to register vessel structures that are represented as centerline graphs. We form a space of good features by iteratively creating new graphs from projected centerline images and by restricting the correspondence search only on branching points (the vertices) of the vessel tree. This algorithm shows good convergence and proves to be robust against deformation changes, which is demonstrated through studies on one phantom and three patients.

1 Introduction

Angiographic imaging is a widely used technique for intravascular interventions. In such treatments a preoperative 3D data set is usually acquired for diagnosis and planning. This data set shows detailed information of the patient's anatomy. 3D data sets are commonly acquired using CTA. During the intervention an intraoperative imaging device captures the current state of placed catheter and anatomy of the patient for navigation. In clinical practice, 2D fluoroscopic projections of the region of interest are acquired lacking spatial resolution compared to the preoperative data sets. Patients suffering from primary liver cancer are frequently treated with Transarterial Chemoembolizations (TACE). Here, in order to apply local chemotherapy and embolizing the blood vessels supporting the tumor, a catheter is inserted into the arterial vasculature in the hip region and guided to the tumor's location using DSAs. The navigation through the vessel system is rather difficult for physicians due to lack of depth perception and

R. Larsen, M. Nielsen, and J. Sporring (Eds.): MICCAI 2006, LNCS 4190, pp. 873–881, 2006.

information about the tumor's location, which can only be visualized once the catheter is near the tumor and contrast injections propagate further down the vessel tree. Registering pre- and intraoperative data sets would allow physicians to view the catheter in 3D together with tumor location and detailed patient anatomy. Much attention has been drawn to the problem of 2D-3D registration of angiographic images. Intensity-based methods register two data sets by creating artificial X-ray projections (Digitally Reconstructed Radiographs, DRR) and optimizing cost functions directly evaluating pixel intensities [1, 2]. Feature-based approaches segment the vessels or extract vessel centerlines in order to use them as features for alignment optimizing distance-based cost functions. The former methods are very accurate but time-consuming due to expensive DRR generation (for our patient data, DRR generation takes approximately 1 second), while the latter ones are fast, robust, but often have to cope with segmentation errors and thus lack of accuracy. Since vessel structures are the dominant features in angiographic images, they are exclusively used for feature-based registration. Research is focusing on determination of corresponding points on vessel structures [3], choice of suitable metrics with (near) projective invariance [4, 5, 6, 7], and derivation of globally converging optimization procedures [8]. Hybrid methods register segmentations of (reconstructed) vasculature using intensity-based methods [9, 10]. All of these works address vessels in neurovascular images where rigidity is preserved or use gating for deformation compensation. To our knowledge, gating-absent 2D-3D registration in deformable regions like organs in the abdomen has not been performed yet. Moreover, the inherent tree property of vessel structures has not been used by these approaches. 2D-3D angiographic registration for liver interventions is an unsolved problem mainly because of two reasons. First, a suitable protocol for CTA to contrast liver arteries is not used in clinical practice. Second, an adequate registration algorithm which addresses the difficult task of aligning deformed vessel structures has not been developed yet. We present a novel one-click method for automatic rigid 2D-3D registration of angiographic images. We introduce a new CT protocol to visualize also liver arteries, which is the only visible structure during the interventional procedure. This protocol enhances the diagnostic value of CTA scans with interventional benefit and introduces a new way of intraoperative visualization. In a first step of the algorithm, 2D and 3D vasculatures are segmented using a combination of smoothing, background removal, and vessel enhancement filters followed by region growing. For the registration, graphs are created from both segmented data sets via a wave propagation algorithm [11] detecting vessel bifurcations as vertices and segments between junctions as edges. The algorithm then initializes one bifurcation correspondence via a-priori information of the patient location and near projective invariance of the vessel diameter. A nonlinear optimization is performed on a reduced parameter space iterating over 3 rotational and 1 translational parameter. Good feature correspondences are iteratively created for the matching by recurrent graph creation of the projected 3D centerline image. As will be shown, the registration algorithm is robust to deformation changes by focusing on the vasculature's bifurcations. Monte Carlo simulations on rigid phantom data and three patient data sets show convergence and robustness of the new algorithm. Graph representations of vessel structures have been used in 3D-3D deformable registration of different hepatic vessel trees [12, 13]. These approaches do not have to cope with projective invariance and can

use angles and lengths for their registration. Moreover, the hepatic vessel trees represent the portal venous system where the diameter of vessels and thus the number of bifurcations is higher compared to the arterial liver tree that is used in our approach.

2 CTA Protocol for Diagnosis and Intervention

The current workflow for TACE involves a three-phase CTA scan of the liver region consisting of native, arterial dominant, and portal-venous phase visualizing mainly the portal venous system, and the hepatic veins. However, during the intervention only arteries are visible in DSA, no portal or hepatic vessel systems, such that until now 2D-3D registration was not possible. We create a strong link between diagnostic radiology and intervention by defining a new protocol for the preoperative scans, introducing one additional run of an *angiographic* phase that visualizes liver arteries (delay times with bolus tracking: 6 (angiographic), 10 ± 2 (arterial dominant), 21 ± 4 (portal-venous) seconds), see fig. 1. The aim is to let the interventionalist benefit from 3D high resolution CTA scans for planning before, and for navigation during the intervention. We have acquired several data sets using a state-of-the-art 64-slice CT imaging device (Siemens Sensation 64). The spatial precision of the acquired scans could be reconstructed to $0.58 \times 0.58 \times 0.6 mm^3/voxel$ in a $512 \times 512 \times (280 - 500)\, voxel$ volume making it possible to extract vessels with a diameter down to $1 - 2mm$. As confirmed by physicians, the additional radiation exposure is acceptable for patients undergoing a TACE treatment. This new scan protocol is used to perform the registration. As a result, paths can be planned and intraoperative enhanced 3D navigation and visualization can be offered. To plan the path (roadmap) through the vessel system to the pathology on the new data set is one major issue for interventionalists. Registering the 3D pre- with the 2D intraoperative data allows to project this plan on the current DSA enabling physicians to discern vessel paths more easily.

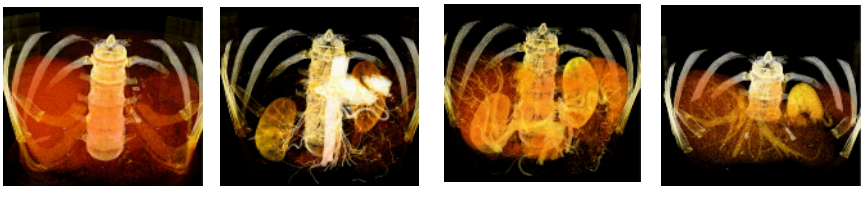

(a) native (b) angiographic (c) art. dominant (d) portal-venous

Fig. 1. The new 4-phase CT protocol

3 Method

The presented method extracts a 3D and a 2D centerline graph from the vessel structures of the angiographic data sets and rigidly registers them using both, geometric and topological information. An initialization detects one point correspondence (the root). Then, an optimization is performed on a four dimensional parameter space combining projection, graph extraction, and cost function evaluation in each iteration.

3.1 Preprocessing

Segmentation. Since contrast agent is applied globally in a CTA scan, its propagation is uniform, but covers less of the vessel tree, opposite to DSA images where contrast is intraarterially applied. Moreover, the diameter of liver arteries is rather small (1-7 pixels), other than in 2D where magnification of the imaging device increases the size of tubular structures. Thus, we use two different methods in 3D and 2D for segmenting the vasculature. The 3D volume of the angiographic scan is smoothed using an anisotropic diffusion filter before the user has to place a seed point at the beginning of the arterial tree to be segmented. A region growing algorithm extracts the vasculature. In 2D, a background removal is performed by applying a bothat filter (closed image minus original image) followed by a multiscale vesselness filter assigning the probability of lying in a tubular structure to each pixel as described in [14]. A region growing algorithm extracts the vessel structure from a placed seed point.

Extraction of Graphs. From the segmented data sets one can easily extract a centerline image by applying thinning algorithms in 3D and 2D [15]. We extend a wave propagation algorithm [11] to cope with loops and use it for graph creation from this centerline. The graph $G = (V,E)$ is created with vertices at branching points of the vessel tree and edges in between (see fig. 2). Points between each bifurcation are sampled and stored as edge labels to keep edge position information. Since the thinning algorithm still introduces some wrong branches due to noise, edges smaller than the vessel diameter (which is also stored in G) are removed with a euclidean distance transform of the segmented data sets. For the same reason and in the same way very adjacent bifurcations are fused together.

3.2 Registration

Rigid 2D-3D registration aims at recovering the 6 degrees of freedom providing the viewing parameters of 2D image capture. The 6 DOFs are also referred to as the extrinsic parameters $[R|t]$ of a perspective projection, $x = PX = K[R|t]X$. $P \in \mathbb{R}^{3\times4}$ projects a homogeneous 3D point X onto a homogeneous 2D point x and can be decomposed into K (intrinsic parameters) and rotation R and translation t (extrinsic parameters). Since the interventional imaging device used (Siemens Axiom Artis) is fully calibrated, K is known. Moreover, distortion has already been compensated for inherently.

For given correspondences between 2D and 3D points ($x_i \leftrightarrow X_i,\ i = 1 \ldots n_1$), the solution to this problem is well-known: Find R,t that minimize the least-squares cost function

$$f_{lsq} = \sum_{i}^{n_1} ||x_i - \Phi_K(R,t,X_i)||^2,$$

where Φ_K is the projecting function with calibration matrix K. In our case, however, corresponding information is not available.

Initialization. State-of-the-art angiographic C-arm devices store lots of information concerning imaging geometry. Each 2D angiogram is provided with the calibration matrix K, a source-to-object (SOD)[1] distance, and an estimated magnification factor (s).

[1] The SOD is actually a source-to-table distance, but is called source-to-object distance in the DICOM header.

Moreover, it can be assumed that an image is acquired approximately from top-view visualizing the patient horizontally lying on the intervention table. With this a-priori information we can assume near projective invariance of centerlines and thus vessel diameters [6]. An initialization step tries to find a 2D correspondence to the bifurcation in 3D with the largest vessel attached, which is called the root. After setting the a-priori information we iteratively translate the 3D graph in x- and y-direction parallel to the image plane such that the root's projection is laid over 2D bifurcations attached to vessels with high diameter. The cost function f_{topo}, described further in this section, is evaluated and the (x,y)-translation yielding the lowest value is chosen. Thus, we find one corresponding vertex and reduce our optimization problem to recovering three rotational parameters (R) and one translational parameter t_{root} along the ray connecting X-ray source position to the projected root on the image plane.

Geometric Registration. 2D-3D registration problems are twofold: recovery of corresponding information and estimation of rigid transformation. Since vessel structures can be interpreted as a number of curves, the well-known Iterative Closest Point (ICP) algorithm could be incorporated for finding both, matches and transformation parameters. Let $C(G,p)$ be a function determining the point of graph G closest to a given point p , the cost function is changed into

$$f_{icp} = \sum_{i}^{n_2} ||C(G_{2D}, \Phi_K(R, t_{root}, X_i)) - \Phi_K(R, t_{root}, X_i)||^2,$$

where $X_j,\ j = 1 \ldots n_2$ are all points representing the 3D vasculature (bifurcations and segment sampling points). Naturally, f_{icp} has many local minima since projected points of one 3D vessel segment could easily be driven to different, not corresponding 2D vessel segments in the optimization process. Moreover, even with outlier detection via an adaptive distance threshold based on statistical analysis, the cost function would yield wrong alignment due to deformation.

If we focus the correspondence search not on all curve points but only on dedicated ones that are likely to be detected in both data sets, we can improve the estimation process. Bifurcation points can be detected in 2D and 3D data sets very easily and represent good descriptors for a projection of vasculature since they are distributed over the whole vessel tree and are distinct to each other. Hence, we restrict our cost function only to these good features, the vertices $\{v_i\}$ of the graphs. Only inner vertices can be used since leaves in the graph account for the end of contrast propagation, which is different in 3D and 2D data sets. Unfortunately, segmentations and hence extracted graphs of the data sets are often very different due to local and global application of contrast agent. Moreover, the projection also produces crossings of vessels that cannot easily be detected and resolved since vessels can also be tangent to each other. This can be dealt with by performing a new graph extraction on the projected graph's centerline image in each iteration. The centerline image is created by drawing the 3D graph as a one-voxel-wide centerline in a volume and projecting the volume with the current imaging parameters.

Topological Registration. Since we deal with graph structures, we can also incorporate topological information in the registration. Due to different segmentation results in 2D

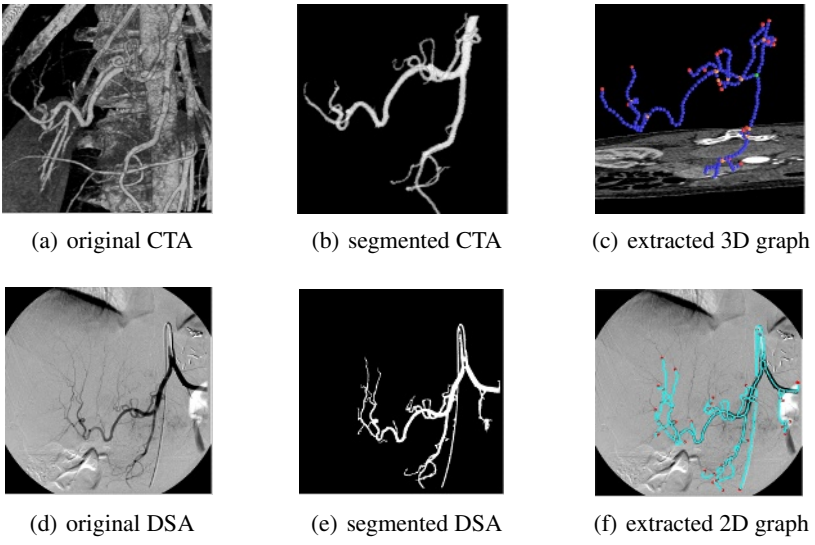

(a) original CTA (b) segmented CTA (c) extracted 3D graph

(d) original DSA (e) segmented DSA (f) extracted 2D graph

Fig. 2. Preprocessing in 3D/2D. (a): volume rendered CTA, (b): segmented vasculature, (c): extracted graph; the green point is the root node, orange points inner, red points outer bifurcation points, blue points represent sampling points of the vessel segments. (d) and (e): original DSA and segmented vasculature.(f): 2D graph (turquoise are sampling, red are bifurcation points).

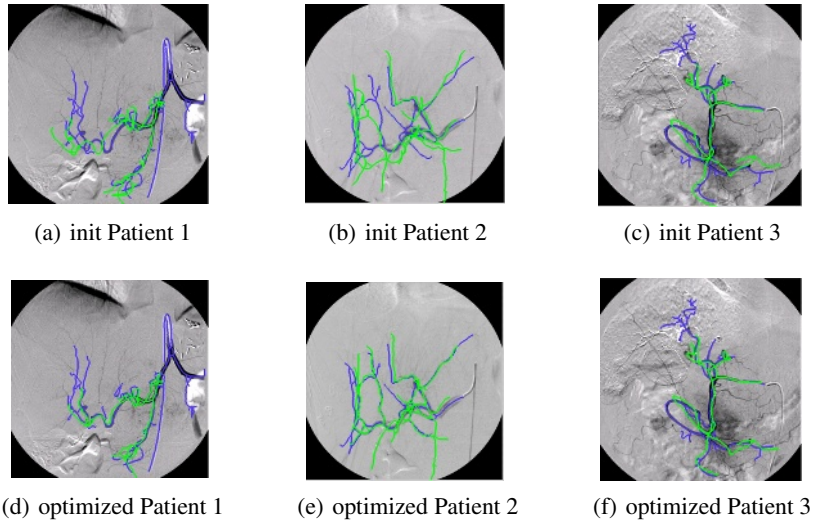

(a) init Patient 1 (b) init Patient 2 (c) init Patient 3

(d) optimized Patient 1 (e) optimized Patient 2 (f) optimized Patient 3

Fig. 3. Diameter initialized and registered pose of all patient data sets.

and 3D, the two graphs to be registered do not fulfill the subgraph property and it is not straightforward to do a topology-based graph matching to register the data. However, topological *tendencies* can be used for registration. The degree of each vertex can be

used as well as a time stamp coming from a breadth first search to penalize wrong bifurcation matches. In order to also involve the geometric meaning of the degree of each vertex, we determine the closest points to small edge segments (curves with up to 5 sampling nodes, we will call them *edgels*) attached to each bifurcation:

$$f_{topo} = \sum_{i}^{n} r_i^{bfs} \cdot r_i^{deg} \cdot ||C(v_j, \Psi_{K,i}(R, t_{root}, G_{3D})) - \Psi_{K,i}(R, t_{root}, G_{3D})||^2 + \sum_{t}^{m} ||C(G_{2D}^{edgel}, \Gamma_{K,t}(R, t_{root}, G_{3D})) - \Gamma_{K,t}(R, t_{root}, G_{3D})||^2,$$

where $\Psi = (v_1^{proj}, \ldots, v_{n_4}^{proj})$ projects the 3D graph G_{3D} with the current parameters R, t_{root}, and extracts a new graph from the projected graph's centerline image starting at the location of the projected root vertex. The resulting 2D graph's inner bifurcation list (without leaves) is returned by Ψ. r_i^{bfs} is the ratio of the normalized breadth first search values of the current bifurcation v_i^{proj} and the closest bifurcation in the 2D graph or its reciprocal if $r_i^{bfs} < 1$. r_i^{deg} is the ratio of the degrees of v_i^{proj} and the closest 2D bifurcation or its reciprocal if $r_i^{deg} < 1$. G_{2D}^{edgel} is a (disconnected) graph representing only bifurcations with edgels attached to them, and Γ returns the sampling nodes $(s_1, \ldots, s_m)$ of the edgels of the projected graph that has been created from the current centerline image. Since the cost function f_{topo} is highly non-linear a Downhill Simplex optimization was chosen.

4 Experiments and Results

Experiments have been carried out on a phantom head showing a rigid vessel structure and on three patient data sets. Ground truth registration has been created by intensity-based registration for the phantom head using Gradient Correlation as similarity measure and manually by physicians for the patient data. The initialization step was successfully performed for each of the data sets. The optimization procedure took 10-20 seconds for phantom and patient data.In order to evaluate the convergence and robustness of the optimization, Monte Carlo simulations have been carried out on all data sets. Random displacements in a range of $\pm 10^\circ$ in rotation angles and $\pm 10mm$ in translation along the axis connecting X-ray source position to root node have been added to the ground truth pose and the registration procedure was invoked. The following table shows standard deviations and root mean square errors (RMS) of 150 trials for each of the four parameters. Patient 1 has few deformation since the DSA was recorded at approximately the same breathing state whereas Patient 2 and 3 have rather large deformation. The larger deviation and RMS value for patient three is due to a more local distribution of the nodes in the DSA and CTA.

	$\sigma_\alpha[^\circ]$	$\sigma_\beta[^\circ]$	$\sigma_\gamma[^\circ]$	$\sigma_t[mm]$	$RMS_\alpha[^\circ]$	$RMS_\beta[^\circ]$	$RMS_\gamma[^\circ]$	$RMS_t[mm]$
Phantom	3.6	1.6	2.6	1.6	3.6	1.7	2.6	2.2
Patient 1	4.1	3.9	0.8	7.7	5.3	4.3	0.8	8.7
Patient 2	1.7	3.8	0.8	9.9	3.3	4.0	0.8	9.9
Patient 3	5.2	7.2	3.3	35.5	5.4	7.2	4.5	60.5

Fig. 3 shows the three patient data sets after initialization (a),(b),(c) and after optimization (d),(e),(f). The blue line shows the extracted 2D graph, the green line the projected 3D graph. As can be observed, the optimization procedure improves the initial alignment up to a deformation of the vessels. Thanks to the new CTA phase, interventionalists can plan the catheter insertion for TACE. At this point, the interventionalists are more interested in a precise rigid 2D-3D registration allowing them to execute their plan, and do not consider a deformable registration as vital. Therefore, the measure of success in this paper is a precise rigid 2D-3D registration up to a final deformation of vasculature

5 Conclusion

We introduce a new CTA scanning protocol for liver interventions resulting in a benefit for interventionalists in terms of depth perception and 3D planning to the diagnostic value of 3D high resolution images. By developing a 2D-3D registration algorithm based on the newly acquired data we enable physicians to transfer planning information to the interventional room. We overcome the difficulty of alignment by conceiving an algorithm, which iteratively generates good features that can be detected easily in 2D and 3D and describe the perspective projection adequately. The combination of geometrical properties of the vasculature like branching point coordinates or vessel diameter with topological properties of the vessel tree using an intuitive graph representation drives the registration process to an optimum quickly and robustly, if a good distribution of bifurcations over the image is provided. According to physicians the accuracy of the registration complies with the goal of plan transfer from 3D to 2D, i.e. from pre- to intraoperative data. Clinical evaluation and introduction of physically meaningful deformation will follow this work in the future.

Acknowledgements. This research was partially funded by an academic grant from Siemens Medical Solutions Angiography/X-Ray division, Forchheim, Germany. The authors would like to thank in particular Klaus Klingenbeck-Regn and Marcus Pfister for their continuous support.

References

1. Kerrien, E., Berger, M.O., Maurincomme, E., Launay, L., Vaillant, R., Picard, L.: Fully automatic 3d/2d subtracted angiography registration. In: MICCAI. (1999) 664–671
2. Turgeon, G.A., Lehmann, G., Guiraudon, G., Drangova, M., Holdsworth, D., Peters, T.: 2d-3d registration of coronary angiograms for cardiac procedure planning and guidance. Med. Phys. **32** (2005) 3737–3749
3. Kita, Y., Wilson, D., Noble, J.: Real-time registration of 3d cerebral vessels to x-ray angiograms. In: MICCAI. (1998) 1125–1133
4. Alperin, N., Levin, D.N., Pelizzari, C.A.: Retrospective registration of x-ray angiograms with mr images by using vessels as intrinsic landmarks. Journal of Magnetic Resonance Imaging **4** (1994) 139–144
5. Feldmar, J., Ayache, N., Betting, F.: 3d-2d projective registration of free-form curves and surfaces. In: Proc. Int'l Conf. of Computer Vision (ICCV). (1995) 549–556

6. Liu, A., Bullitt, E., Pizer, S.: 3d/2d registration via skeletal near projective invariance in tubular objects. In: MICCAI. (1998) 952–963
7. Chan, H., Chung, A., Yu, S., Wells, W.: 2d-3d vascular registration between digital subtraction angiographic (dsa) and magnetic resonance angiographic (mra) images. In: Proc. of the IEEE International Symposium on Biomedical Imaging. Volume 1205 of LNCS., IEEE (2004) 708–711
8. Florin, C., Williams, J., Khamene, A., Paragios, N.: Registration of 3d angiographic and x-ray images using sequential monte carlo sampling. In: Computer Vision for Biomedical Image Applications, First Int'l Workshop, CVBIA '05. Volume 3765 of LNCS., Springer (2005) 427–436
9. Hipwell, J., Penney, G., McLaughlin, R., Rhode, K., Summers, P., Cox, T., Byrne, J., Noble, J., Hawkes, D.: Intensity based 2d-3d registration of cerebral angiograms. IEEE Trans. on Medical Imaging (TMI) **22** (2003) 1417–1426
10. Vermandel, M., Betrouni, N., Palos, G., Gauvrit, J.Y., Vasseur, C., Rousseau, J.: Registration, matching, and data fusion in 2d/3d medical imaging: Application to dsa and mra. In: MICCAI. (2003) 778–785
11. Zahlten, C., Jürgens, H., Peitgen, H.O.: Reconstruction of branching blood vessels from ct-data. In: Eurographics Workshop of Visualization in Scientific Computing, Springer (1994) 161–168
12. Charnoz, A., Agnus, V., Malandain, G., Forest, C., Tajine, M., Soler, L.: Liver registration for the follow-up of hepatic tumors. In: MICCAI. (2005) 155–162
13. Aylward, S., Jomier, J.: Rigid and deformable vasculature-to-image registration: A hierarchical approach. In: MICCAI. (2004) 829–836
14. Frangi, A.F., Niessen, W.J., Vincken, K.L., Viergever, M.A.: Multiscale vessel enhancement filtering. In: MICCAI. (1998) 130–137
15. Palágyi, K., Sorantin, E., Balogh, E., Kuba, A., Halmai, C., Erdöhelyi, B., Hausegger, K.: A sequential 3d thinning algorithm and its medical applications. In: Proc. Int'l Conf. Information Processing in Medical Imaging (IPMI). Volume 2028 of LNCS., Springer (2001) 409–415